

# UC Irvine

## UC Irvine Previously Published Works

### Title

Evaluating Open Source Software for 3D Imaging and Morphing in Cosmetic and Reconstructive Surgery.

### Permalink

<https://escholarship.org/uc/item/1b05062v>

### Journal

The Laryngoscope, 131(2)

### ISSN

0023-852X

### Authors

Hong, Ellen M  
Hakimi, Amir A  
Ho, David  
[et al.](#)

### Publication Date

2021-02-01

### DOI

10.1002/lary.28857

### Copyright Information

This work is made available under the terms of a Creative Commons Attribution License, available at <https://creativecommons.org/licenses/by/4.0/>

Peer reviewed

## How I Do It

# Evaluating Open Source Software for 3D Imaging and Morphing in Cosmetic and Reconstructive Surgery

Ellen M. Hong, BA ; Amir A. Hakimi, BS ; David Ho, BS; Behrooz A. Torkian, MD;  
Brian J.F. Wong, MD, PhD

**Key Words:** Photogrammetry, 3D, open source, morphing, mesh, print, model.

*Laryngoscope*, 131:299–303, 2021

## INTRODUCTION

Stereophotogrammetry is the process of using multiple photographs of a single subject to create a stereo pair and record depth for composite three-dimensional (3D) model generation. Commercial stereophotogrammetry systems have become increasingly popular in clinical practice, providing 3D imaging for surgical education, operative planning, and patient evaluation. Currently, the largest barrier to 3D stereophotogrammetry is its cost, which is significantly more expensive than its two-dimensional (2D) predecessors. Commercial systems can cost as much as \$70,000.<sup>1</sup> The question remains: can the same task be accomplished using readily available software at a lower cost?

This study is the first to create and morph 3D human models using open source and web-based software and ubiquitous photography hardware. This economical price point can lead to increased accessibility and thus broader adoption of 3D modelling for surgical planning and education. The generated models are compatible with commercial 3D printers, further enriching educational and surgical value.

From the Beckman Laser Institute & Medical Clinic (E.M.H., A.A.H., D.H., B.J.W.), University of California – Irvine, Irvine, California, U.S.A.; Torkian Facial Plastic Surgery, Lasky Clinic Surgical Center (B.A.T.), Beverly Hills, California, U.S.A.; Department of Biomedical Engineering (B.J.W.), University of California – Irvine, Irvine, California, U.S.A.; and the Department of Otolaryngology - Head and Neck Surgery, School of Medicine (B.J.W.), University of California - Irvine, Orange, California, U.S.A.

Additional supporting information may be found in the online version of this article.

Editor's Note: This Manuscript was accepted for publication on May 21, 2020.

The authors have no funding or conflicts of interest to declare.

**Meeting Information:** This manuscript was presented as an oral presentation at the Triological Society Combined Sections Meeting in Coronado, California, USA January 23-25, 2020.

Send correspondence to Brian J.F. Wong, MD, PhD, 1002 Health Sciences Road, Irvine, CA 92612. E-mail: bjwong@uci.edu

DOI: 10.1002/lary.28857

## METHODS

A schematic of the following workflow can be found in Fig. 1.

### Photography

Images were captured on a solid-color background in a room with diffuse, white natural light to minimize shadowing effects. Nine angles were demarcated on the transverse Frankfort plane with respect to the midsagittal plane: 90°, 67.5°, 45°, 22.5°, 0°, -22.5°, -45°, -67.5° and -90°; and five angles of axes were used in the sagittal plane with respect to the transverse Frankfort plane: 60°, 30°, 0°, -30°, -60°, totaling 45 images (Fig. 2). These positions were selected based on pre-operative facial plastic surgery photography guidelines set forth by the Institute of Medical Illustrators.<sup>2</sup> While this allows the maximization of the number of photographs accepted by the software in an evenly spaced manner, these positions are merely a guideline and a description of the method used by the researchers. An iPhone 6S (Apple, Cupertino, CA) and a Canon EOS 6D (Canon, Melville, NY) were used manually to capture clear and in-focus photographs of the subject. To prevent image distortion previously described with iPhone images, the field of view was set to 2x digital zoom with the subject's head occupying half the screen. Thirty-second videos using both camera systems were also captured of the subject at three angles of axes in the sagittal plane with respect to the transverse Frankfort plane (30°, 0°, -30°) as the subject rotated 180° from profile to profile at each angle.

The subject was also photographed using the Vectra XT (Canfield Scientific, Inc., Parsippany, NJ) to compare the proposed workflow against a widely-used commercial model.

### 3D Mesh/Texture Construction

The mesh that defines shape in 3D modelling, and the texture which provides color information, were generated using 3DF Zephyr Free (3DFZF) (3D Flow, Verona, Italy). The mesh was exported as an "alias wavefront object" (.obj) file and the texture as a "JPEG" (.jpg) file. The resulting models can be seen in Fig. 3.

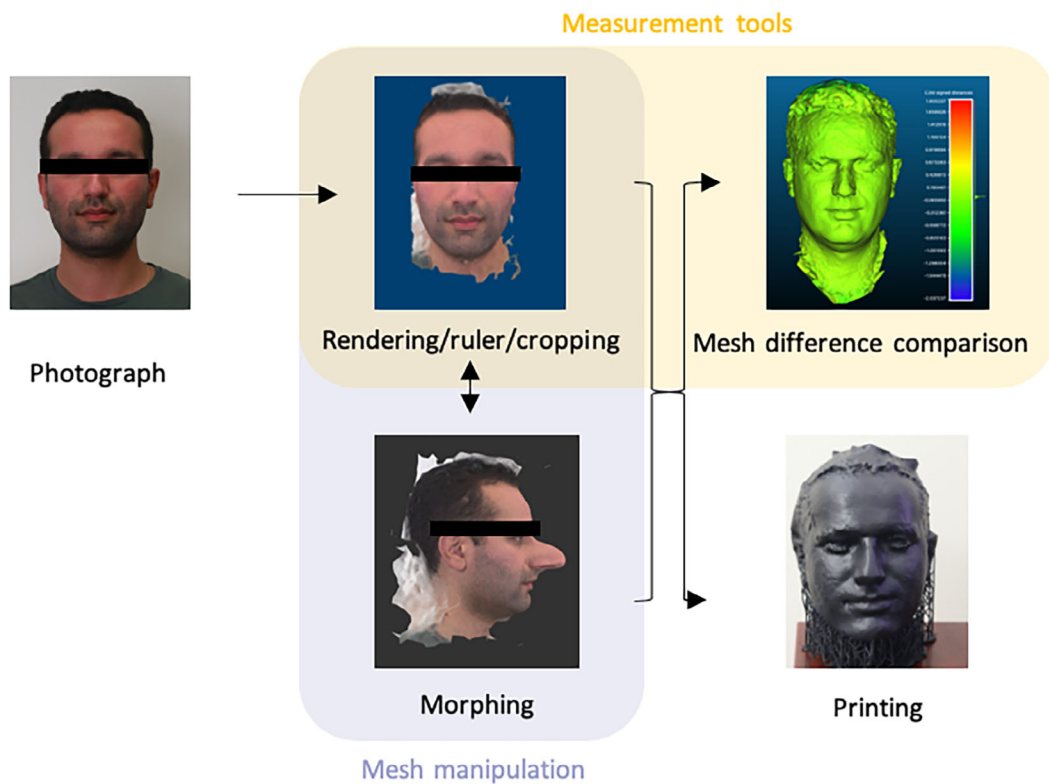


Fig 1 An overview of the workflow. [Color figure can be viewed in the online issue, which is available at [www.laryngoscope.com](http://www.laryngoscope.com).]

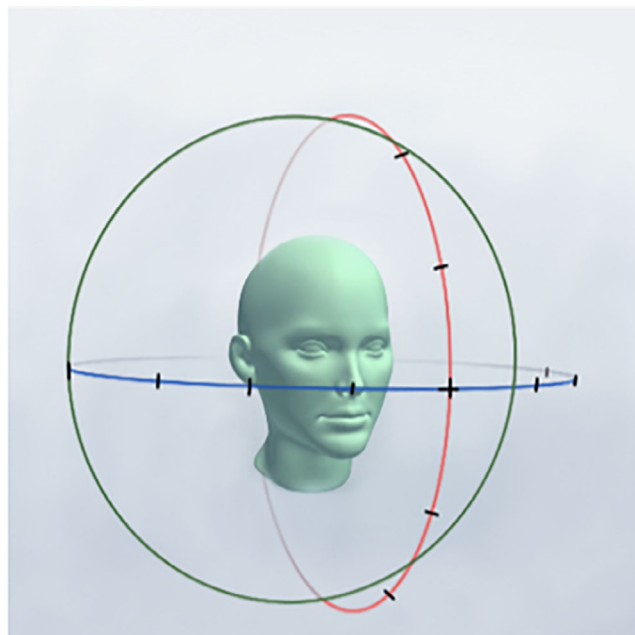


Fig 2 Indications of angles at which photographs were taken to generate the 3D model. The black tick marks demarcate the positions the camera was held. [Color figure can be viewed in the online issue, which is available at [www.laryngoscope.com](http://www.laryngoscope.com).]

### 3D Mesh Manipulation

The mesh and texture were both uploaded to the SculptGL (Ginier, 2015) web application. A video demonstrating the

following is included (Video S1). The mesh was reoriented to align with pre-set perspectives internal to the software including frontal, profile, superior, and inferior views.

The menu under the “Sculpting and Painting” header was used to manipulate the 3D mesh. Within the “Tool” drop-down menu, the “Drag” option most closely replicates the “liquify” option in Photoshop. The “radius” scale adjusts area of effect, permitting manipulation of the selected pixels. Once morphing was complete, the scene was exported. Upon exportation, the edited file can be reuploaded to 3DFZF to be measured with the “Quick Measurement” tool.

### Measurements

**Caliper.** Measurements with a caliper were performed to compare the fidelity of the 3D mesh to reality. In order to measure the created mesh in 3DFZF, the “Quick Measurements” tool was used to select the beginning and endpoints of each measurement on the mesh. Because the resulting distance defined by the software is an unknown unit, several measurements of facial landmarks were taken using the software. These measurements were replicated on the subject using calipers, and the ratios between the corresponding measurements were found. The average of the ratios was calculated to determine the scale of the software measurements versus caliper measurements. The mean ratio measurements were then multiplied by each internal measurement from 3DFZF to scale the model to life-size. A paired t-test was then used to determine if the two measurements were significantly different (Table I).

**CloudCompare.** The software CloudCompare (Paris, France) was used to compare the fidelity of the 3DFZF mesh to that of the Vectra XT. Due to variability in the rendering of hair, the meshes were cropped to a significant facial feature, the nose. The files were finely aligned, and the mesh differences were computed in the software. The mean Gaussian distribution was internally calculated.

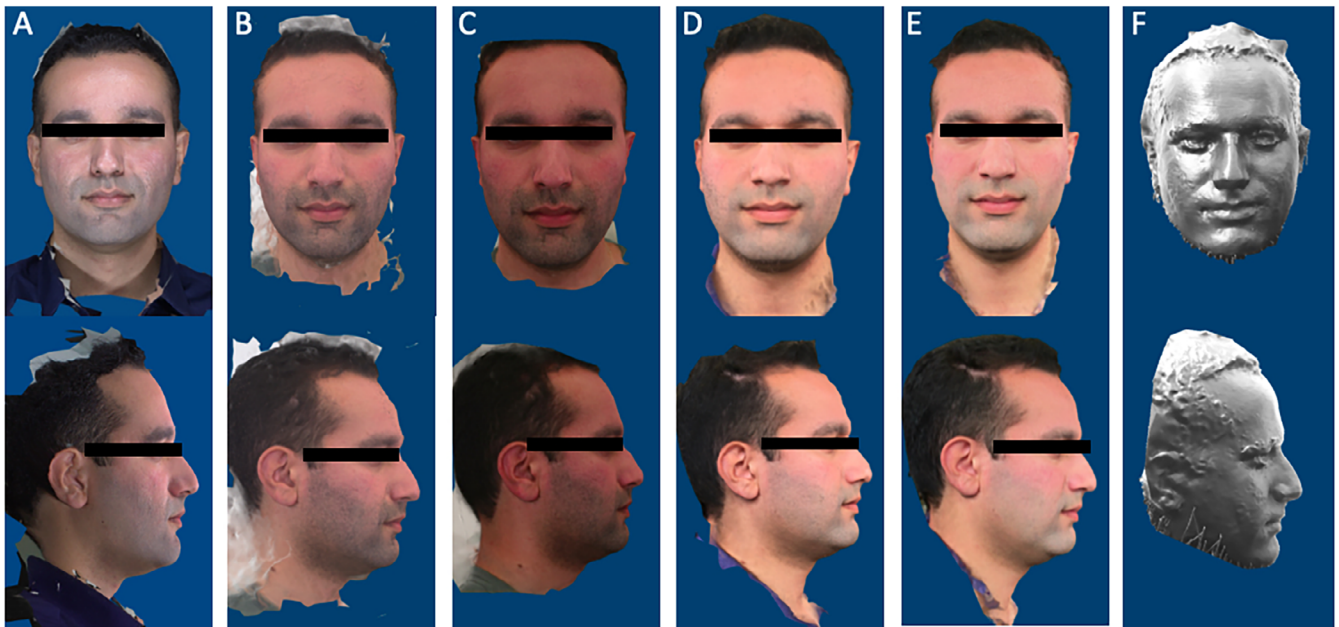


Fig 3 Frontal and profile views of the 3D models rendered from (A) commercial system, (B) DSLR stills, (C) DSLR video, (D) iPhone stills, (E) iPhone video, and (F) 3D printing. [Color figure can be viewed in the online issue, which is available at [www.laryngoscope.com](http://www.laryngoscope.com).]

Table I.

Caliper Measurements of the Subject's Facial Landmarks were Compared to those Internally Generated in the Free Software and to Measurements Taken From a Printed 3D Model. The Measurements Were Scaled and Entered in a Paired t-test with the Caliper Measurements to Determine the Statistical Significance of the Difference.

Facial Landmarks	Caliper of human subject (mm)	Vectra Scaled (x 1.004)	DSLR Stills Scaled (x 112.48)	DSLR Video Scaled (x 91.55)	iPhone Stills Scaled (x 34.38)	iPhone Video Scaled (x 35.20)	Model Scaled (x1.522)
<b>Intercanthal distance</b>	32.28	35.37	33.68	35.96	35.36	34.83	37.60
<b>Philtrum height</b>	15.61	17.98	18.23	18.27	18.63	18.47	15.62
<b>Lower lip midline height</b>	10.69	10.04	11.11	10.81	11.20	10.73	9.240
<b>Radix to nasal tip</b>	58.67	56.41	56.85	57.86	59.85	57.75	55.99
<b>Nasal tip width</b>	25.21	25.17	23.55	24.61	26.46	25.14	25.57
<b>Columellar length</b>	18.20	15.91	14.40	14.90	13.31	14.67	17.75
<b>Width of Alar flare</b>	34.36	35.32	40.10	34.39	34.87	35.33	37.10
<b>P-Value</b>		.8394	.7433	.7811	.5345	.7526	.6072

### 3D Printing

A consumer-grade 3D printer, Form 2 (Formlabs, Somerville, MA), was used to 3D print the meshes generated by 3DFZF. The "Size" tool in the accompanying software allows for changes to scale, using the average of the ratios calculated from the measurements to scale to life-size. Caliper measurements of a scaled 3D print based on the generated model were also tested against caliper measurements of the human subject to assess fidelity (Table I).

## RESULTS

### Caliper

The null hypothesis is that the true mean differences between the caliper measurements and the scaled 3DFZF measurements is equal to 0. To reject that null

hypothesis, the *P*-value from the paired t-test must be  $<.05$ . The *P*-values of the paired t-test between the caliper measurements and the scaled 3DFZF measurements are shown in Table I, indicating that the difference between the caliper measurements and the scaled 3DFZF measurements in all 4 photogrammetry techniques are not statistically significant. The difference between the caliper measurements of the 3D print and those of the human subject was also found to be not statistically significant ( $P = .6072$ ).

### CloudCompare

Each mesh generated in 3DFZF was compared with that from the Vectra system using the CloudCompare software (Fig. 4). The resulting colors represent the

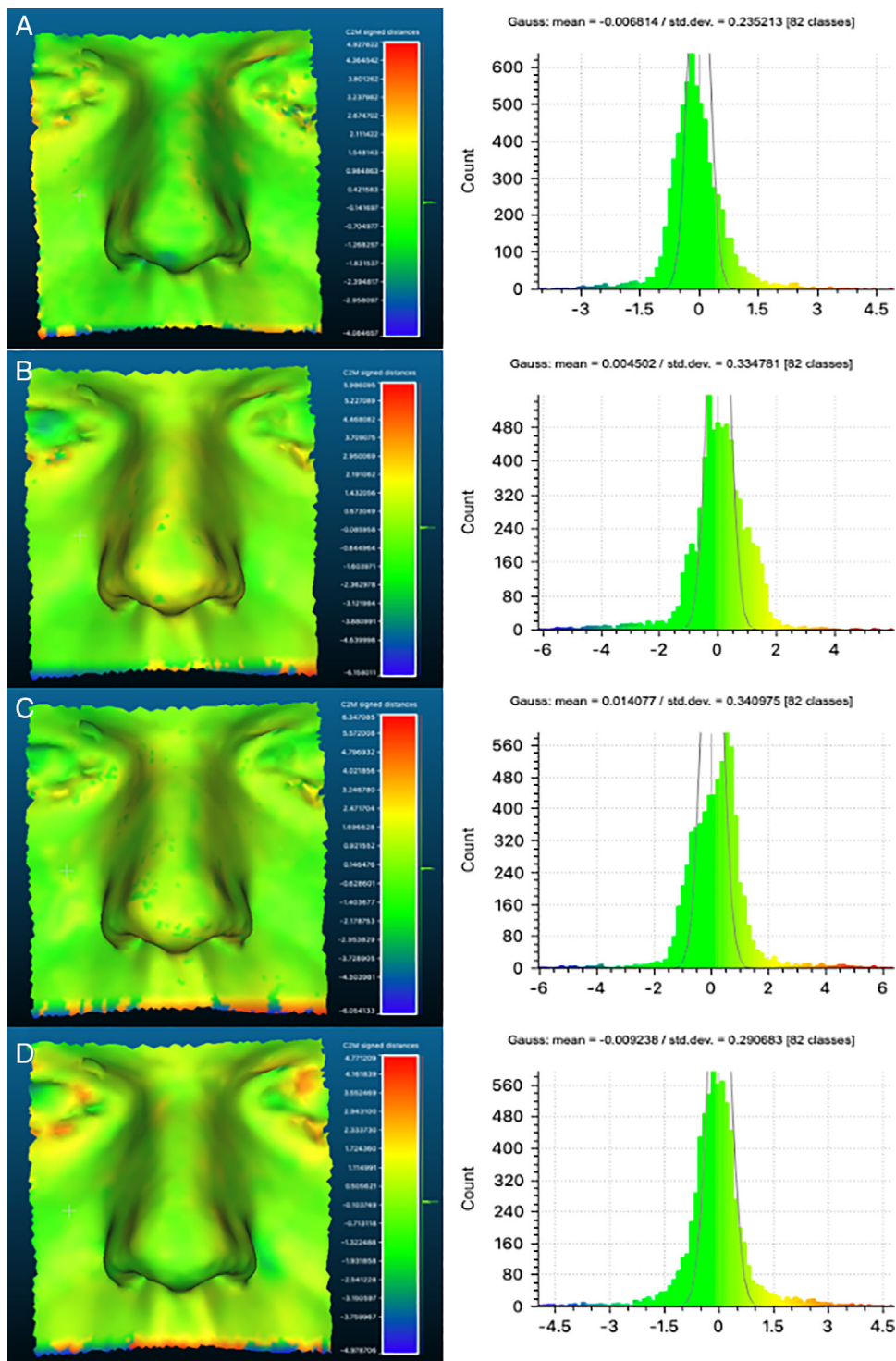


Fig 4 Distances were computed between aligned meshes using CloudCompare. The commercial system was compared against the (A) DSLR stills, (B) DSLR video, (C) iPhone stills, (D) iPhone video. The histograms depict the respective Gaussian distributions and denote the mean and standard deviation. [Color figure can be viewed in the online issue, which is available at [www.laryngoscope.com](http://www.laryngoscope.com).]

distance between the meshes, where blue is a negative distance, green is no distance, and red is a positive distance. The means and standard deviations of the Gaussian distributions of the differences are shown in Fig. 4.

## DISCUSSION

This study establishes a workflow using entirely free software with a human subject as a model. Furthermore, the reconstructions can produce colored textures, more closely replicating reality.

A major advantage to our proposed method is its low cost. As smartphones are ubiquitous and DSLRs are the standard in surgeon's offices, the cost of this proposed workflow is limited to the cost of the camera system, compared to \$10,000<sup>3</sup> or even \$70,000<sup>1</sup> of proprietary hardware. Furthermore, this software is less expensive than many 2D software packages like Photoshop. Finally, the ability to incorporate video footage, as opposed to multiple images, decreases the temporal burden of the surgeon and patient during pre- or post-operative imaging.

Another advantage of this workflow stems from its production of 3D meshes that are scalable and accurate. The difference between the mesh measurements established by 3DFZF and the caliper measurements obtained by the researchers was not found to be statistically significant, indicating the mesh's high fidelity to reality. This allows surgeons to accurately recreate a subject's facial features, providing a better reference for surgery. Before and after 3D imaging permits quantitative measurements of outcomes, which is rarely done now with 2D photography. Mesh comparisons verify that the meshes rendered from 3DFZF is comparable to that rendered using the Vectra XT. The Vectra has been previously validated as a clinical and anthropometric tool, and is likely the most commercially successful system.<sup>4</sup> However, 3dMD, a widely used 3D surface imaging system, has been considered a "gold standard" for commercial facial stereophotogrammetry.<sup>5</sup> Future studies comparing meshes rendered from 3DFZF against those

from 3dMD would better validate the use of the proposed method.

## CONCLUSION

With the imaging and analysis method defined in this study, it is possible to render and morph 3D models of human subjects with appropriate color grading without software costs. A surgeon would only need a computer and a digital recording device in order to enhance the surgical planning process and provide in depth information to patients. It would be seamless and cost effective to not only upgrade one's practice from a 2D-based method to 3D, but also introduce a form of digital editing. The proposed workflow offers a low-cost method of generating and morphing 3D patient models to aid in education and planning for facial plastic and reconstructive surgeries.

## BIBLIOGRAPHY

1. Lee S. Three-dimensional photography and its application to facial plastic surgery. *Arch Facial Plast Surg* 2004;6:410–414.
2. Photography S. Rhinoplasty and septorhinoplasty photography. *J Vis Commun Med* 2007;30:135–139.
3. Tzou CHJ, Artner NM, Pona I, et al. Comparison of three-dimensional surface-imaging systems. *J Plast Reconstr Aesthetic Surg* 2014;67:489–497.
4. Metzler P, Sun Y, Zemann W, et al. Validity of the 3D VECTRA photogrammetric surface imaging system for craniomaxillofacial anthropometric measurements. *Oral Maxillofac Surg* 2014;18:297–304.
5. Knoops PGM, Beaumont CAA, Borghi A, et al. Comparison of three-dimensional scanner systems for craniomaxillofacial imaging. *J Plast Reconstr Aesthetic Surg* 2017;70:441–449.